

Electronic Supplementary Information (ESI)

A Reactive Molecular Dynamics Study on the Anisotropic Sensitivity in Single Crystal

α -Cyclotetramethylene Tetranitramine

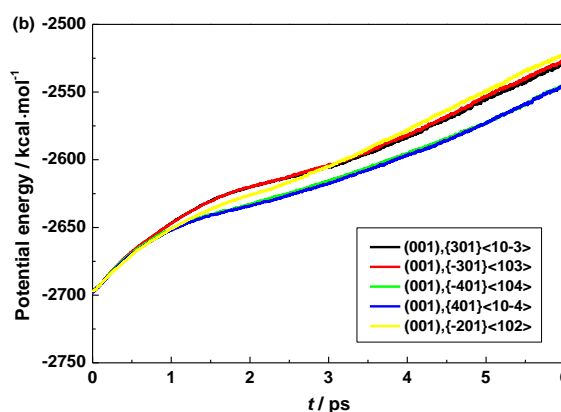
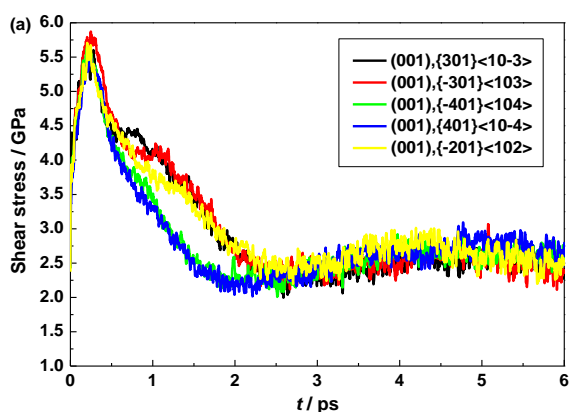
(Ting-Ting Zhou, Yan-Geng Zhang, Jian-Feng Lou, Hua-Jie Song, Feng-Lei Huang)

Table S1 The averaged full stress tensors for the seven uniaxially compressed structures after NVT-MD relaxation (unit: GPa)

Shock plane	P	P_{xx}	P_{yy}	P_{zz}	P_{xy}	P_{xz}	P_{yz}
(010)	9.549	8.544	13.447	6.657	0.181	0.237	0.089
(001)	10.164	7.638	10.431	12.421	-0.124	-0.117	-0.212
(100)	10.305	11.994	9.304	9.616	-0.082	0.148	0.110
(110)	10.218	12.396	9.411	8.845	0.013	0.017	0.080
(011)	10.097	7.716	10.509	12.065	-0.033	0.035	0.127
(111)	10.099	8.935	9.163	12.200	0.007	0.779	0.122
(101)	10.484	9.397	10.068	11.985	-0.363	0.913	-0.082

Table S2. Bond order cutoff values for various atom pairs. The algorithm of molecule recognition in the fragment analysis uses these values.

	C	H	O	N
C	0.55	0.40	0.60	0.30
H		0.55	0.40	0.55
O			0.65	0.40
N				0.55



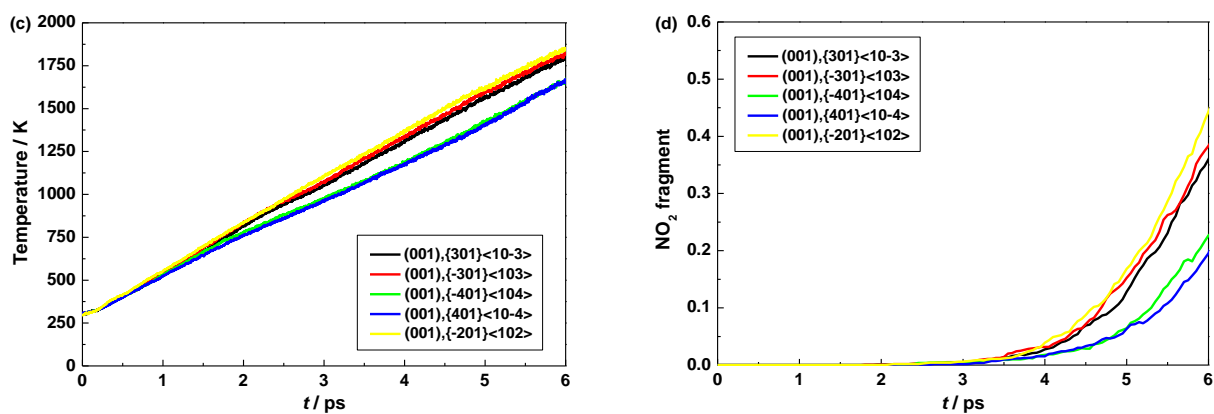


Fig. S1 Time evolutions of shear stress (a), potential energy per HMX molecule (b), temperature (c), and NO₂ fragment per HMX molecule (d) for the five possible slip systems along shock direction normal to the (001) plane during shear simulations.

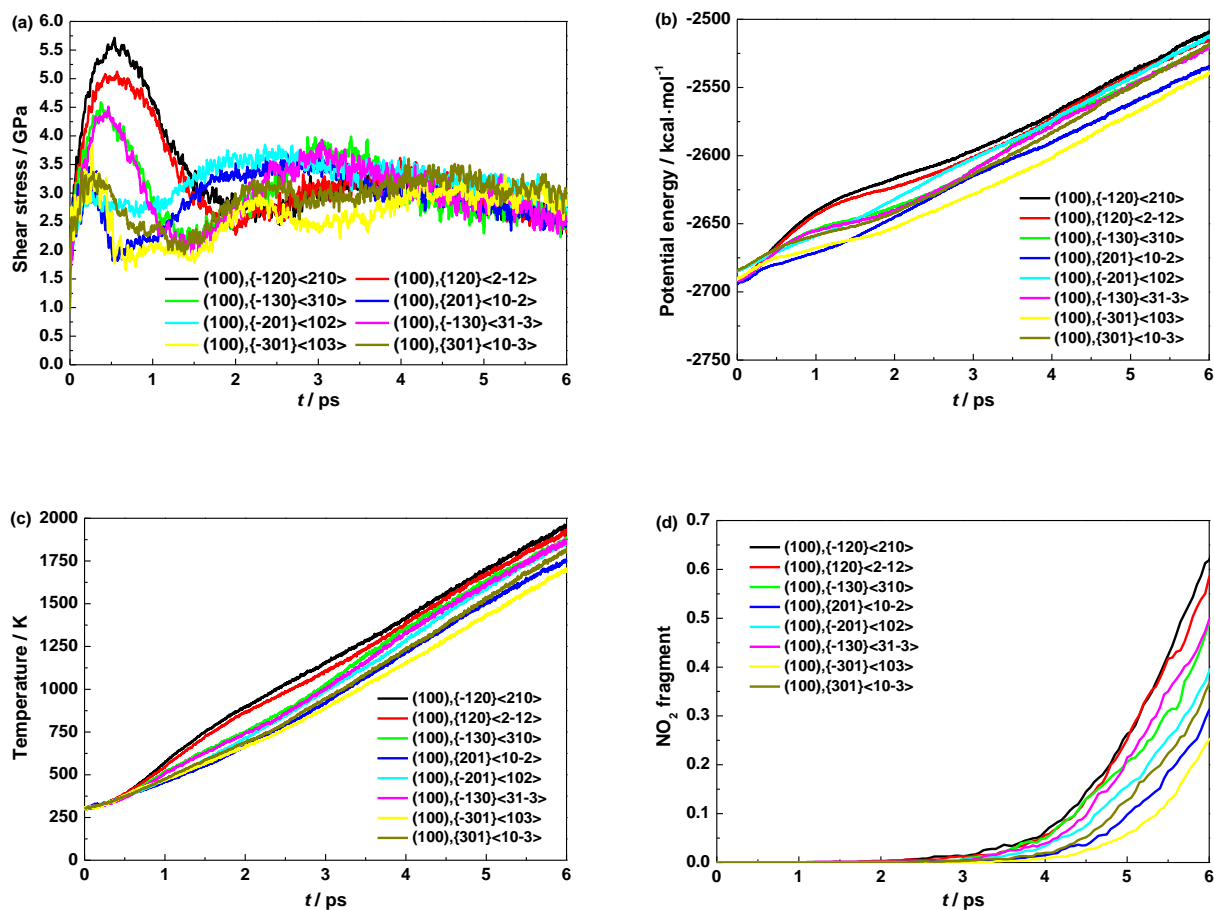


Fig. S2 Time evolutions of shear stress (a), potential energy per HMX molecule (b), temperature (c), and NO₂ fragment per HMX molecule (d) for the eight possible slip systems along shock direction normal to the (100) plane during shear simulations.

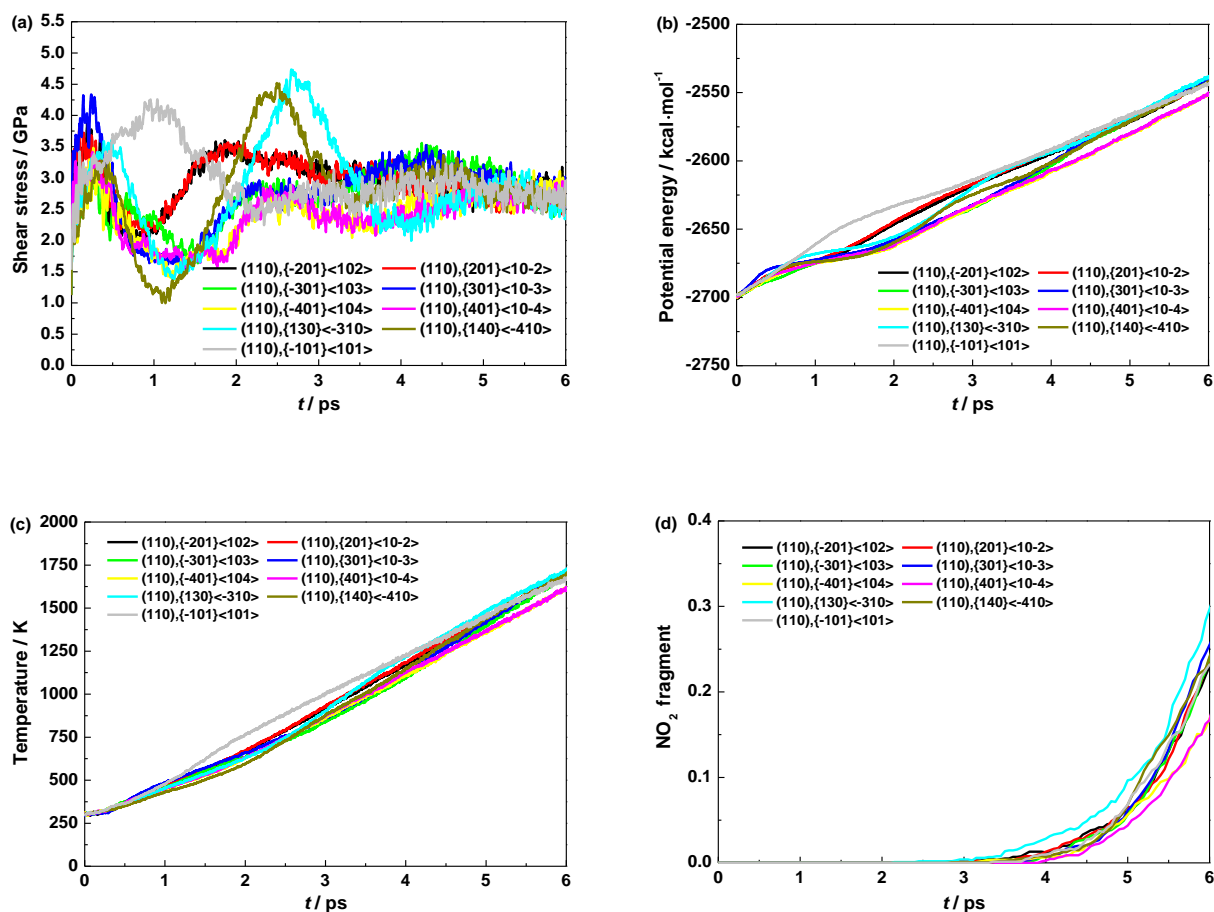
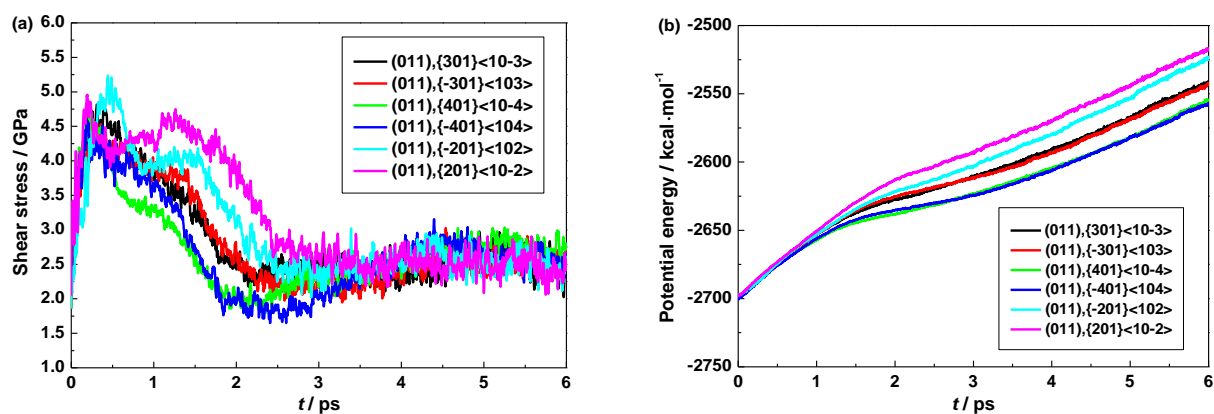


Fig. S3 Time evolutions of shear stress (a), potential energy per HMX molecule (b), temperature (c), and NO₂ fragment per HMX molecule (d) for the eight possible slip systems along shock direction normal to the (110) plane during shear simulations.



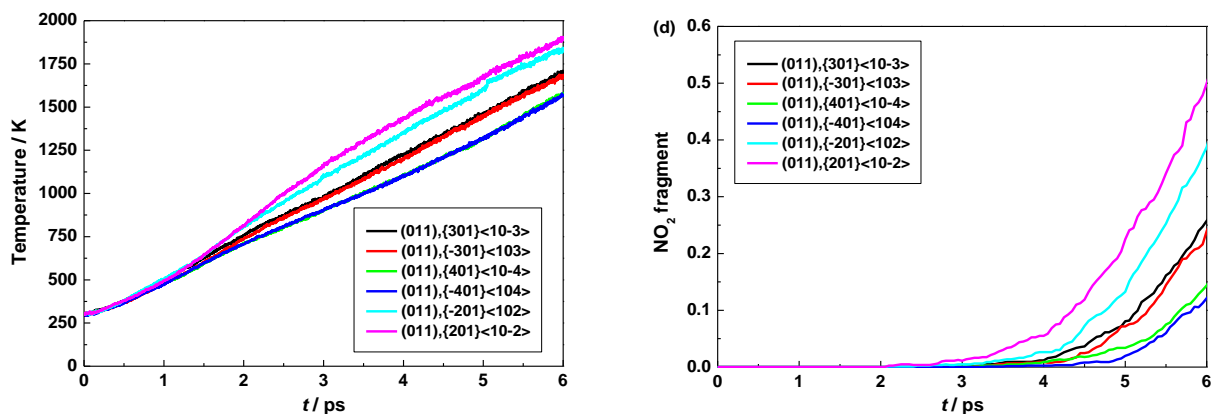


Fig. S4 Time evolutions of shear stress (a), potential energy per HMX molecule (b), temperature (c), and NO₂ fragment per HMX molecule (d) for the eight possible slip systems along shock direction normal to the (011) plane during shear simulations.

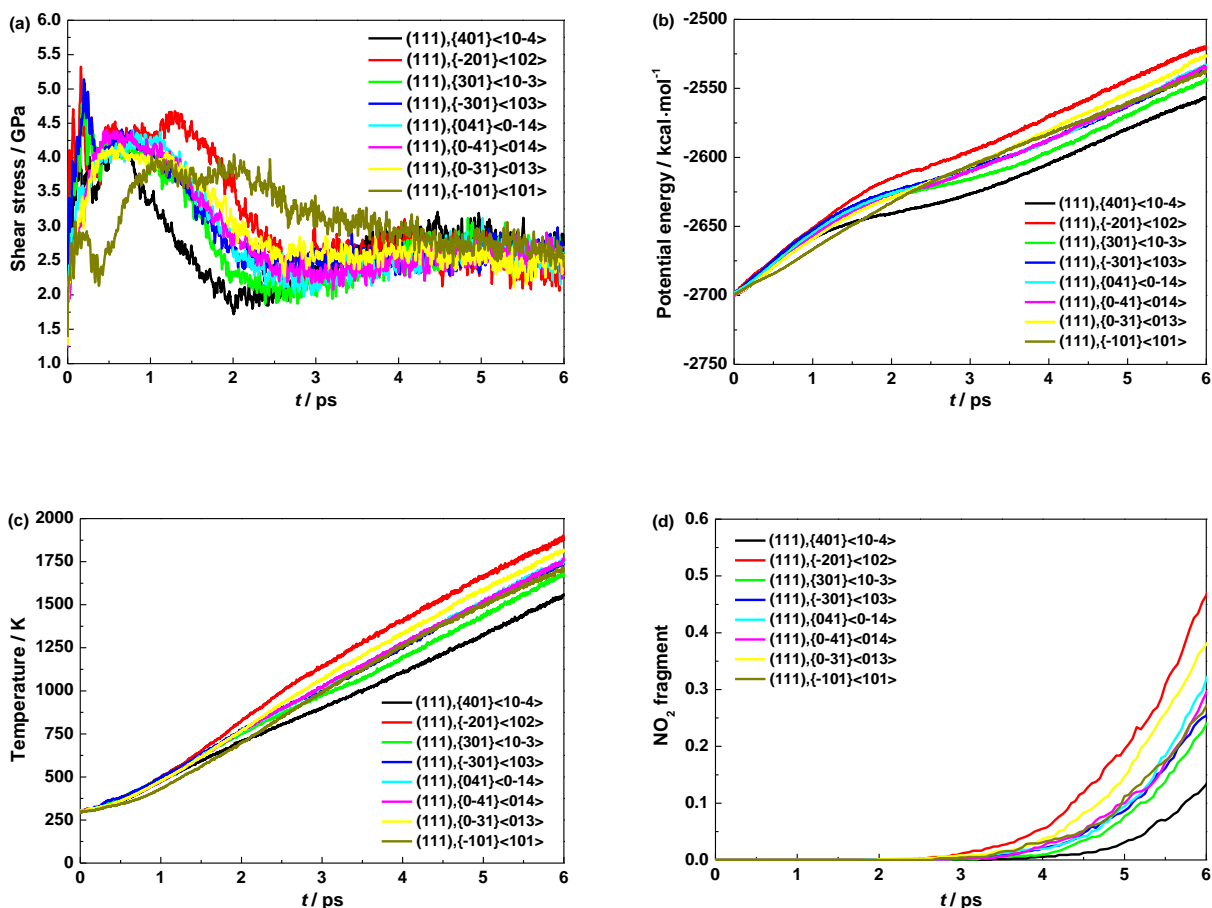


Fig. S5 Time evolutions of shear stress (a), potential energy per HMX molecule (b), temperature (c), and NO₂ fragment per HMX molecule (d) for the eight possible slip systems along shock direction normal to the (111) plane during shear simulations.

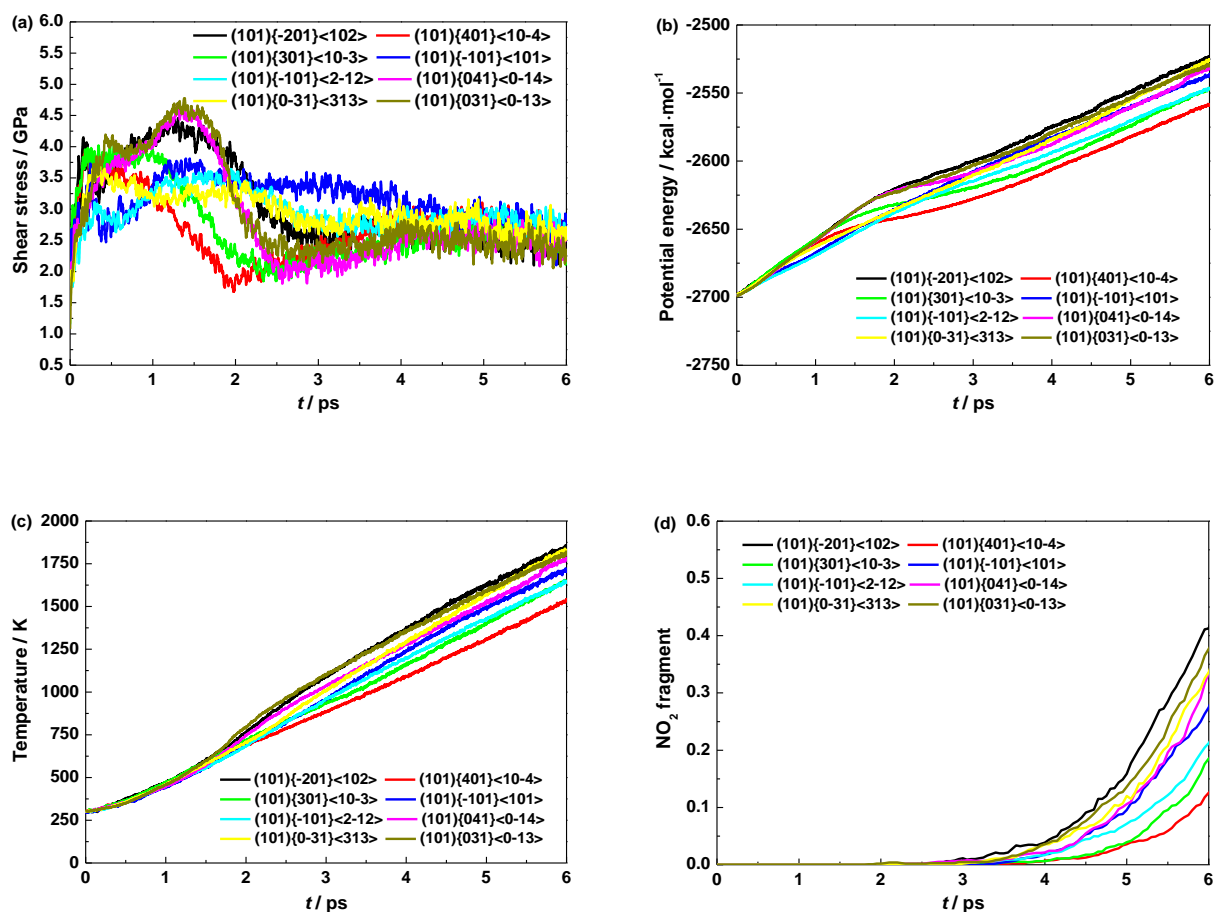
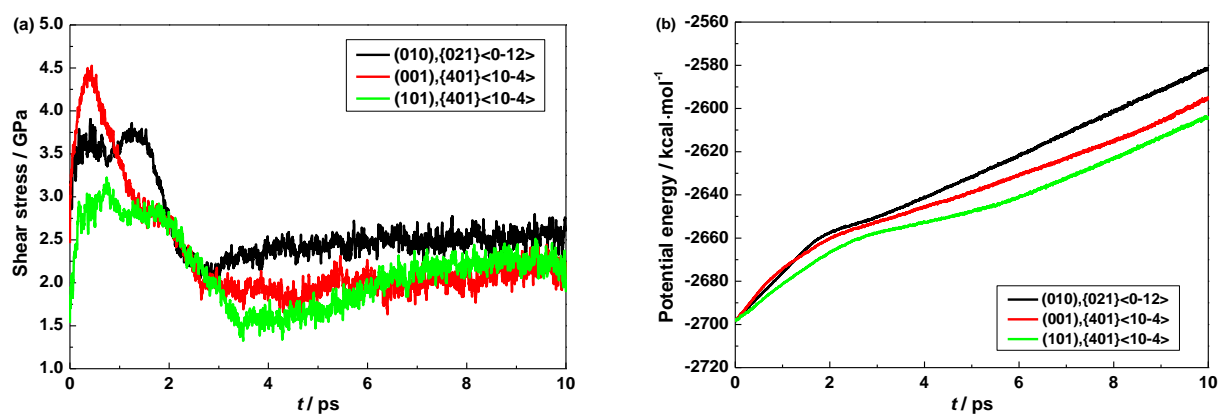


Fig. S6 Time evolutions of shear stress (a), potential energy per HMX molecule (b), temperature (c), and NO₂ fragment per HMX molecule (d) for the eight possible slip systems along shock direction normal to the (101) plane during shear simulations.



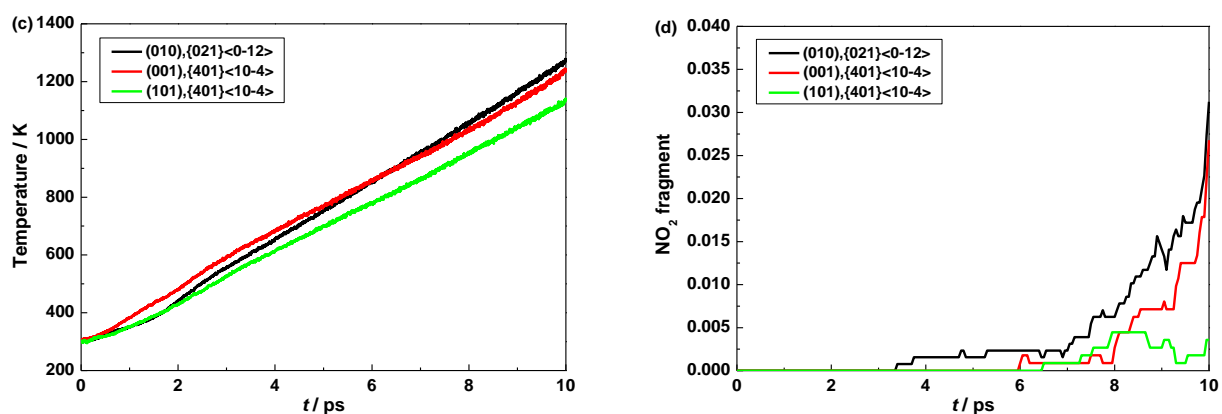


Fig. S7 Time evolutions of shear stress, potential energy per HMX molecule, temperature, and NO₂ product per HMX molecule for the (010), (001), and (101) shock planes during shear simulations at shear rate 0.25 ps⁻¹

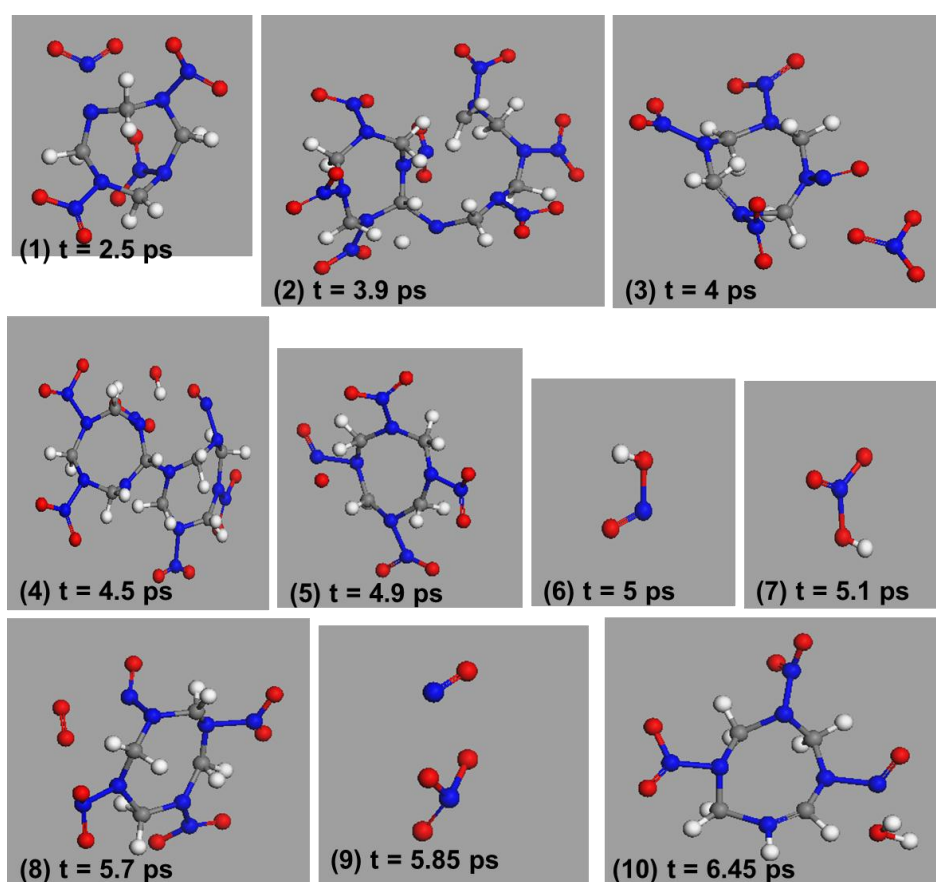


Fig. S8 The snapshots of reaction products at the first time of their appearances from the MD trajectories for the (010) shock plane. $C_4H_8O_8N_8$ (297) \rightarrow $C_4H_8O_6N_7$ (1283) + O_2N (1284); (2) $C_4H_8O_6N_7$ (1281) + $C_4H_8O_8N_8$ (1245) \rightarrow $C_8H_{15}O_{14}N_{15}$ (1349) + H (1350); (3) $C_4H_8O_{10}N_9$ (1344) \rightarrow O_3N (1362) + $C_4H_8O_7N_8$ (1361); (4) $C_8H_{16}O_{12}N_{14}$ (1427) \rightarrow $C_8H_{15}O_{11}N_{14}$ (1522) + HO (1523); (5) $C_4H_8O_8N_8$ (707) \rightarrow $C_4H_8O_7N_8$ (1680) + O (1681); (6) O_2N (1444) + H (1718) \rightarrow HO_2N (1740); (7) H (1459) + O_3N (1653) \rightarrow HO_3N (1792); (8) $C_4H_8O_9N_8$ (2275) \rightarrow O_2 (2334) + $C_4H_8O_7N_8$ (2333); (9) O_4N_2 (2157) \rightarrow ON (2532) + O_3N (2533); (10) $C_4H_{10}O_6N_7$ (3315) \rightarrow H_2O (3402) + $C_4H_8O_5N_7$ (3401). The numbers in brackets are molecule ID.

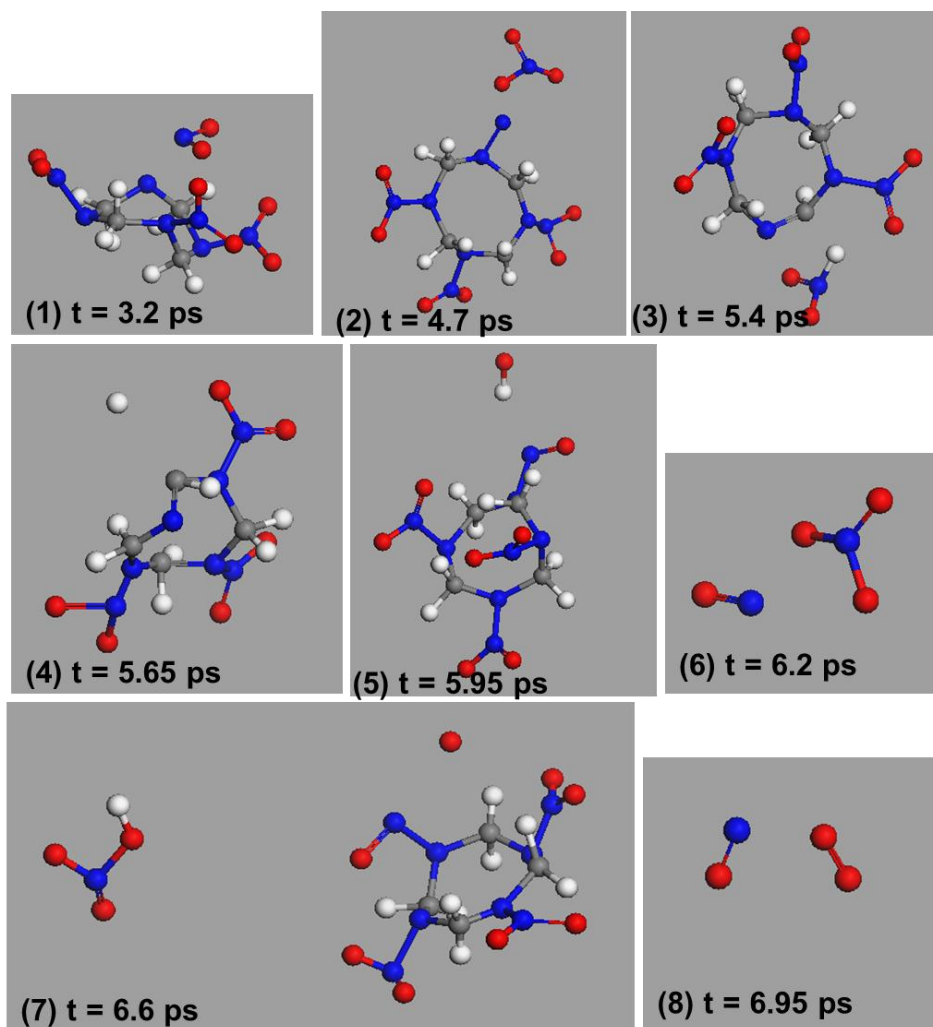


Fig. S9 The snapshots of reaction products at the first time of their appearances from the MD trajectories for the (101) shock plane. (1) $C_4H_8O_8N_8$ (474) $\rightarrow C_4H_8O_6N_7$ (1121) + O_2N (1122); (2) $C_4H_8O_9N_9$ (1149) $\rightarrow C_4H_8O_6N_8$ (1168) + O_3N (1169); (3) $C_4H_8O_8N_8$ (1272) $\rightarrow C_4H_7O_6N_7$ (1290) + HO_2N (1291); (4) $C_4H_8O_6N_7$ (1302) $\rightarrow C_4H_7O_6N_7$ (1388) + H (1389); (5) $C_4H_9O_8N_8$ (1493) $\rightarrow C_4H_8O_7N_8$ (1519) + HO (1520); (6) O_4N_2 (1490) $\rightarrow ON$ (1669) + O_3N (1670); (7) $C_4H_8O_8N_8$ (1108) $\rightarrow C_4H_8O_7N_8$ (2136) + O (2137), O_2N (1152) + HO (1520) $\rightarrow HO_3N$ (2084); (8) O_3N (2374) $\rightarrow O_2$ (2435) + ON (2434). The numbers in brackets are molecule ID.

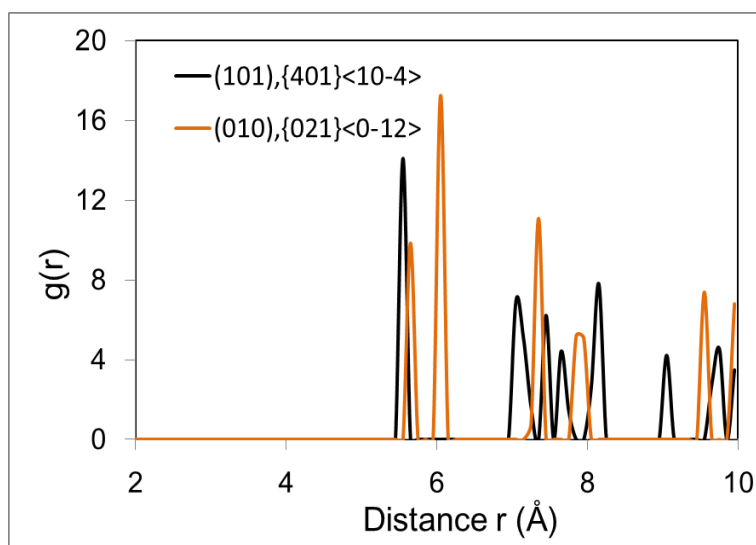


Fig. S10 The radial distribution function $g(r)$ based on the molecular center of mass for the (010) and (101) shocked systems after energy minimization